



Cobalt-chromium-enriched medium ameliorates shear-stressed endothelial cell performance



Mariana Issler Pinheiro Machado^a, Anderson Moreira Gomes^a, Marcel Ferreira Rodrigues^a,
Thais Silva Pinto^a, Célio Júnior da Costa Fernandes^a, Fábio J. Bezerra^a,
Willian Fernando Zambuzzi^{a,b,*}

^a Department of Chemistry and Biochemistry, Bioscience Institute, Sao Paulo State University, UNESP, Campus Botucatu, Botucatu, São Paulo, Brazil

^b Electron Microscopy Center, IBB, UNESP, Botucatu, SP, Brazil

ARTICLE INFO

Keywords:

Biomaterials
Implants
Cobalt
Chromium
Endothelial cell
Blood vessel

ABSTRACT

Angiogenesis is a relevant mechanism to be considered for the success of bone healing, even considering endosseous implantable devices, providing adequate delivery of substances necessary for the cell viability and bone *de novo* deposition. Within the repertoire of metal-based implantable alloys, cobalt-chromium (CoCr) has emerged with very interesting properties for biomedical applications. Additionally, we have shown that released molecules from implants devices are able to modulate cells away and because that we hypothesized these released molecules might act on endothelial cells. In order to better address this issue, we investigated the effect of Co-Cr-enriched medium on endothelial cells (HUVECs), considering a biological model subjecting those cells to shear-stress to partially mimic the physiological environment and further allow investigating intracellular pathways responsible to drive cytoskeletal rearrangement, cell viability and extracellular matrix (ECM) remodeling processes. Considering the analysis of the metalloproteinases (MMPs) activities, our data indicates an intense ECM remodeling in response to CoCr-enriched medium suggesting some role on angiogenesis once ECM remodeling is prerequisite to cell growth. This was better addressed by revealing its involvement on modifying both mRNA expression and protein levels of members of the MAPK family. Additionally, the expression of CDK4 gene was modulated within the cell response to Co-Cr-enriched medium, while the modulation in the expression of P15 and P21 indicates an important regulatory mechanism required. Overall, our results demonstrate that trace of CoCr elements triggers decisive intracellular signaling in shear-stressed endothelial cells, suggesting influence on angiogenesis-related mechanism and they bring novel insights to explain the biological activity of CoCr as it has been emerged as interesting biomedical materials within the medical and dentistry fields.

1. Introduction

As an alternative to implants within medicine and dentistry fields, titanium (Ti) alloys have been used for more than decades, but studies with other biomaterials such as the cobalt-chromium (Co-Cr) alloy have been performed due on their mechanical strength and also considering its biocompatibility when into human tissues and these both characteristics are of extreme importance for alternative biomaterials [1]. Taking these lessons into account, an ideal biomaterial should presents characteristics able to favor the adequate interaction with the host tissue and interfering on their osseointegration [2]. Thus, it sounds relevant to evaluate the cellular behavior in response to cobalt-chromium (Co-Cr), mainly considering the template of analysis widely used

to define previously the biological properties of titanium alloys showing the cellular responses related to their growth and differentiation processes [3]. Additionally, it has been reported the cytotoxicity of cobalt on fibroblast and its ability to trigger inflammatory mediators [4], and because that the cicatrization peri-implant as well as the homeostasis from the host bone might be affected by the presence of these materials [5,6]. Thus, strategies are used to better assimilate the biomaterial to the host tissue, and e.g. nanopography might facilitates the osseointegration process [3,7,8].

Tissue healing peri-implant requires hierarchical involvement of different types of cells, such as mesenchymal stem cells and immunological cells, which harmonically provides adequate environment to drive the osseointegration of those implantable devices. On this

* Corresponding author at: Department of Chemistry and Biochemistry, Biosciences Institute/IBB-UNESP, P.O. Box: 510, 18618-970, Rubião Jr, Botucatu, São Paulo, Brazil.

E-mail address: wzambuzzi@ibb.unesp.br (W.F. Zambuzzi).

<https://doi.org/10.1016/j.jtemb.2019.04.012>

Received 8 November 2018; Received in revised form 25 March 2019; Accepted 23 April 2019

0946-672X/ © 2019 Elsevier GmbH. All rights reserved.

sense, it is already discussed that different cells equally respond differently to the biomaterial's surface [9,10]. In addition to the importance of the success of osseointegration, angiogenesis is relevant and needs to be better considered during bone healing surrounding the implanted devices providing prompt delivery of molecules necessary for the bone *de novo* deposition [11,12]. Considering the endothelium tissue, the lumen of the blood vessels is constituted by a laminar monolayer of endothelial cells, which they are constantly exposed to blood flow forces [13], requiring responses to the mechanotension generated by the shear stress. On this context, endothelial cells paracrine respond for the tissue homeostasis and their relevance on osteogenesis has been addressed [14].

Over the last few years, we have shown an interesting repertory of intracellular molecules able to predict the viability and metabolism of bone cells [2,15–19], highlighting a metabolism map of specific signaling pathways cascade and reprogramming gene expression. Specifically to the cobalt-chromium alloys, we have previously shown that they are able to release active molecules when in solution, which dynamically interacts with cells and triggers specific intracellular signals. Based on these results, we suggested cobalt-chromium able to affect and interfere on surrounding tissue [18], so it is probable that this cobalt-chromium-enriched medium might modulate endothelial cells as well and overall contribute with bone tissue healing at peri-implant region. However, there are few studies showing the effects of Co-Cr on the behavior of endothelial cells, even considering the importance of them during tissue healing process [10].

Importantly, endothelial cells have emerged presenting important modulatory role within tissue, mainly taking into account their capacity to respond to chemical mediators (cytokines, hormones, etcetera), as well as to hemodynamic forces generated by the blood flow itself as shear stress, triggering intracellular processes called "mechanosignaling" [20,21], maintaining their viability through biochemical signal [22]. The mechanosignaling process arises sequential and hierarchical steps - initially cells receive physical forces or stimulus (shear-stress); sensing occurs via cellular structures, triggering signal transduction via signaling molecules; then a transmission and propagation of the signal occurs, when this activate "cellular receptors" and finally a physiological response [23]. Basically, endothelial shear stress (SS) is a force present tangentially to the luminal surface of the blood vessel and is generated when the blood flow acts on the endothelial cells and modulates their biological activity [24], involving activation of several cascades of biochemical and genetic signaling [25]. Considering endothelial cells, these processes are associated with the dynamics of rearrangement of the cytoskeleton [26,27], cell-cell junctions [28], focal adhesion platforms (such as the proteins FAK and Src) [29] and requires transmembrane proteins activation as well [30], culminating on their alignment and functions [31]. In this aspect, we have shown previously that a circuit of mechanical tensional forces differentially requires FAK, Src, as well as PI3K and AKT [32]. We have also suggested this pathway upstream to important mechanism related with endothelial cell viability, able to activate NOS2 and modulate VEGF expression. In order to better address the biological performance of endothelial cells challenged with CoCr-enriched medium, it is necessary consider a biological model where endothelial cells are also experimentally respond to shear-stress, mimicking physiological issues.

Based on the above-mentioned, our study evaluates the behavior of shear-stressed human umbilical vein endothelial cells (HUVEC) responding to cobalt-chromium-enriched medium, investigating intracellular parameters responsible to drive cell viability, such as cytoskeletal rearrangement and ECM remodeling processes.

2. Material and methods

2.1. CoCr alloys and reagents

The metallic CoCr-based discs were gently donated by the S.I.N.

Table 1
Expression primers sequences and qPCR conditions.

Gene	Primer	5'-3' Sequences	Reaction's Conditions
MMP2	Forward	AGCTCCCGAAAAGATTGATG	95 °C – 15 s; 60 °C – 30 s; 72 °C – 30 s
	Reverse	CAGGGTGTGGCTGAGTAGAT	95 °C – 15 s; 60 °C – 30 s; 72 °C – 30 s
MMP9	Forward	CACGCACGACGCTTCCA	95 °C – 15 s; 60 °C – 30 s; 72 °C – 30 s
	Reverse	AAGCGGTCTGGCAGAAAT	95 °C – 15 s; 60 °C – 30 s; 72 °C – 30 s
TIMP1	Forward	CCGCAGCGAGGAGTTTCTC	95 °C – 15 s; 60 °C – 30 s; 72 °C – 30 s
	Reverse	GAGCTAAGCTCAGGCTGTTCCA	95 °C – 15 s; 60 °C – 30 s; 72 °C – 30 s
TIMP2	Forward	CGACATTATGGCAACCTATCA	95 °C – 15 s; 60 °C – 30 s; 72 °C – 30 s
	Reverse	GGGCCGTGTAGATAAAGCTATATCC	95 °C – 15 s; 60 °C – 30 s; 72 °C – 30 s
RECK	Forward	TGCAAGCAGGCATCTTCAA	95 °C – 15 s; 60 °C – 30 s; 72 °C – 30 s
	Reverse	ACCGAGCCATTTCATTCTG	95 °C – 15 s; 60 °C – 30 s; 72 °C – 30 s
COL1A1	Forward	AACCAAGGCTGCAACTGGA	95 °C – 15 s; 60 °C – 30 s; 72 °C – 30 s
	Reverse	GGCTGAGTAGGTTACACGCAGG	95 °C – 15 s; 60 °C – 30 s; 72 °C – 30 s
ERK1	Forward	AACAGGCTCTGGCCACCCAT	95 °C – 15 s; 60 °C – 30 s; 72 °C – 30 s
	Reverse	GCAGCGCCTCCCTTGCTAGA	95 °C – 15 s; 60 °C – 30 s; 72 °C – 30 s
JNK1	Forward	AAAGGTGGTGTGTTTGTCCAGGT	95 °C – 15 s; 60 °C – 30 s; 72 °C – 30 s
	Reverse	TGATGATGGATGCTGAGAGCCATTG	95 °C – 15 s; 60 °C – 30 s; 72 °C – 30 s
AKT	Forward	CAGCGCGCCGGAAGGAC	95 °C – 15 s; 60 °C – 30 s; 72 °C – 30 s
	Reverse	GACGCTACAGGCTCCTCTC	95 °C – 15 s; 60 °C – 30 s; 72 °C – 30 s
FAK	Forward	TCAGTCTCAGACAATCTCTGG	95 °C – 15 s; 60 °C – 30 s; 72 °C – 30 s
	Reverse	CTGAAGCTTGACACCCTCGT	95 °C – 15 s; 60 °C – 30 s; 72 °C – 30 s
SRC	Forward	CAACACAGAGGGAGACTGGT	95 °C – 15 s; 60 °C – 30 s; 72 °C – 30 s
	Reverse	AGCTTCTTCATGACCTGGGC	95 °C – 15 s; 60 °C – 30 s; 72 °C – 30 s
P38	Forward	GAGAAGTCCGGTTACTTA	95 °C – 15 s; 60 °C – 30 s; 72 °C – 30 s
	Reverse	ATGGGTACACAGATACACAT	95 °C – 15 s; 60 °C – 30 s; 72 °C – 30 s
P15	Forward	GGGACTAGTGGAGAAGGTGC	95 °C – 15 s; 60 °C – 30 s; 72 °C – 30 s
	Reverse	CATCATCATGACCTGGATCGC	95 °C – 15 s; 60 °C – 30 s; 72 °C – 30 s
P21	Forward	GCTGCCGAAGTCAGTTCCTT	95 °C – 15 s; 60 °C – 30 s; 72 °C – 30 s
	Reverse	ATCTGTCATGCTGGTCTGCC	95 °C – 15 s; 60 °C – 30 s; 72 °C – 30 s
CDK4	Forward	CTCTAGTCTGGCCCTG	95 °C – 15 s; 60 °C – 30 s; 72 °C – 30 s
	Reverse	GCAGGGATACATCTCGAGGC	95 °C – 15 s; 60 °C – 30 s; 72 °C – 30 s
GAPDH	Forward	AGGCCGGTGTGAGTATGTC	95 °C – 15 s; 60 °C – 30 s; 72 °C – 30 s
	Reverse	TGCCGTGCTC ACCACCTTCT	95 °C – 15 s; 60 °C – 30 s; 72 °C – 30 s
ACTB	Forward	ACAGAGCCTCGCTTTGC	95 °C – 3 s; 55 °C – 8 s; 72 °C – 20s
	Reverse	GCGGGGATATCATCATCC	95 °C – 3 s; 55 °C – 8 s; 72 °C – 20s
18S	Forward	CGGACAGGATTGACAGATTGATAGC	95 °C – 3 s; 55 °C – 8 s; 72 °C – 20s
	Reverse	TGCCAGAGTCTCGTTATTCG	95 °C – 3 s; 55 °C – 8 s; 72 °C – 20s

(São Paulo, SP, Brazil). Ripa buffer (R0278), Phosphatase inhibitor cocktail 2 (P5726), bovine serum albumin (A7906), gelatin (48723), triton X100 (9284) were purchased from Sigma Chemical Co. (St. Louis, MO, USA). Gotaq qPCR master mix (A6002) was purchased from PROMEGA (Madison, Wisconsin, EUA). The following antibodies were purchased from Cell Signaling (Danvers, MA, USA): Cofilin (D59) Antibody (#3318, 19 kDa); PhosphoCofilin (Ser3) Antibody (#3311, 19 kDa); Src (#2109, 60 kDa); Akt Antibody (#9272, 69 kDa); and JNK (46,54 kDa) (Phospho-MAPK Family Antibody Sampler Kit #9910); GAPDH (14C10) Rabbit mAb (#2118, 37 kDa).

2.2. Cell line and culture conditions

Human Umbilical Vein Endothelial Cells (HUVECs; ATCC, Manassas, Virginia, USA) immortalized were maintained in RPMI, containing antibiotics (100U/mL penicillin, 100 mg/mL streptomycin) and 10% (v/v) Fetal Bovine Serum (Nutricell, Campinas, SP, Brazil). Cells were maintained in an incubator at 37 °C, 5% CO₂, and 95% humidity.

2.3. CoCr-enriched medium

In order to prepare the CoCr-enriched medium [both dual acid-etching (DAE) treating surface (named w/DAE) and the machined surfaces (named wo/DAE)], the experimental alloys (n = 6) were incubated in cell culture media (RPMI) without FBS up to 24 h at 37 °C, 5% CO₂, and 95% humidity [0.2 g/mL (w/v); ISO 10993:2016]. CoCr-enriched medium contains molecules released from those metallic alloys and might affect the biology of endothelial cells. To test this

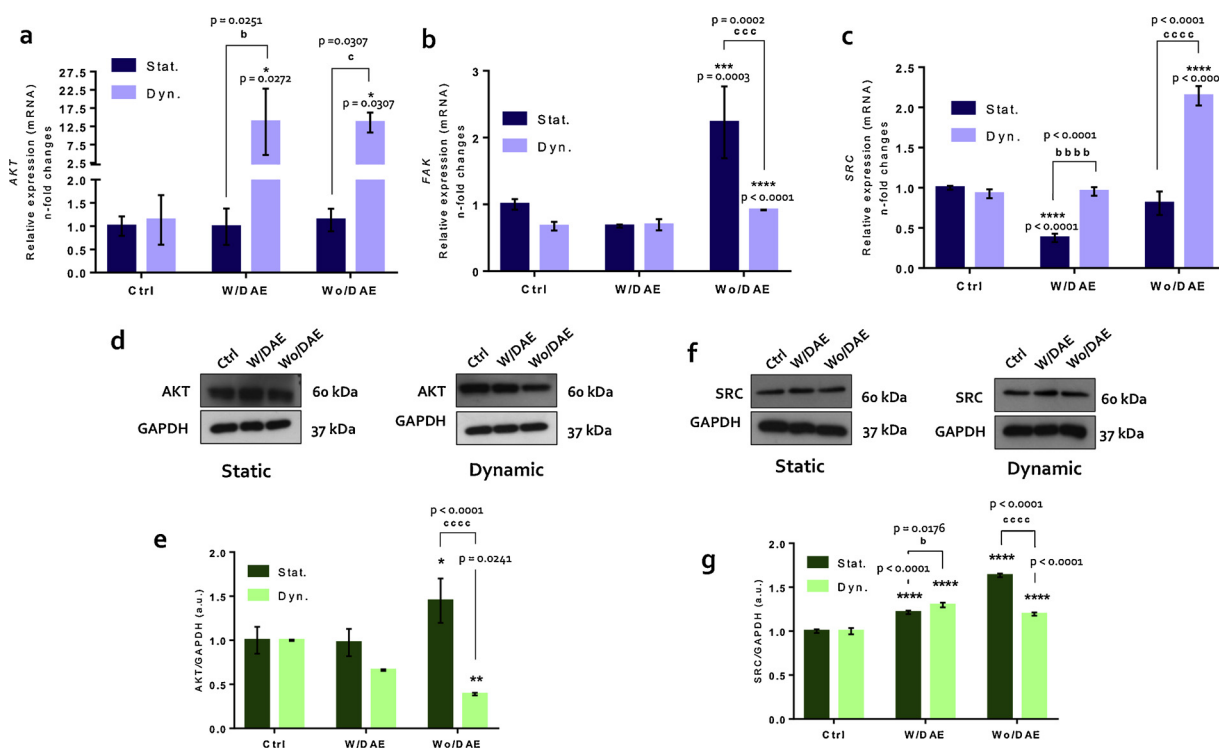


Fig. 1. Survival signaling. The survival panorama was evaluated firstly by qPCR technology, and the genes AKT (a), FAK (b) and SRC (c) were modulated by CoCr-enriched medium. The statistical analyses were performed using two-way ANOVA, with further Sidak's test for multiple comparisons. Significances were when * $p = 0.0272$ (W/DAE vs Dyn.), * $p = 0.0307$ (Wo/DAE vs Dyn.) for AKT; *** $p = 0.0003$, **** $p < 0.0001$ for FAK and **** $p < 0.0001$ for SRC. Additionally, differences were also considered comparing the effects of different surfaces concomitant to shear-stress: ^b $p = 0.0251$ and ^c $p = 0.0307$ for AKT and ^{bbb} $p < 0.0001$ and ^{cccc} $p < 0.0001$ for SRC. Protein profile was also shown by using western blotting technology: AKT (d,e) and SRC (f,g). Representative blottings are displayed, and the graphs represent arbitrary values obtained by the densitometry of the bands, which they were normalized by the average values of the respective GAPDH bands (loading control). * $p = 0.0241$; ** $p = 0.0020$ for AKT and **** $p < 0.0001$ for SRC. Moreover, significances were when ^{cccc} $p < 0.0001$ (AKT) and ^b $p = 0.0176$, ^{cccc} $p < 0.0001$ (SRC). To normalize the data obtained from qPCR technique, we have used 3 reference genes GAPDH, β -actin and 18S.

hypothesis, CoCr-enriched medium was further used to treat the endothelial cells before they are subjected (or not) to the mechanical forces of the shear-stress, as mentioned previously [21,32,33].

2.4. Shear stress

The shear stress was applied in HUVECs previously seeded in the periphery area of modified 100-mm of diameter, where previously 60-mm culture dishes were bonded onto the centered bottom of 100-mm culture dishes using medical silicone and thereafter the this modified dishes were sterilized using UV light for 15 min, as described by dela Paz [34]. The adherent cells were maintained in RPMI up to semi-confluence was reached, at 37 °C, in a humidified atmosphere containing 5% CO₂. The CoCr-enriched medium was used to challenge monolayers of endothelial cells, which they were further subjected to orbital shear-stress up to 72 h at 37 °C in the presence of CO₂ using an SK-O180-Pro Digital Orbital Shaker (SCIOLOGEX, Rocky Hill, CT, EUA). Shear stress protocols respected a rotation frequency of 100 rpm in according to the formula: $\tau_{max} = a\sqrt{\rho\eta(2\pi f)^3}$, where ρ = density and η = viscosity of the culture media and a = orbital rotation radius. Considering our experimental condition, Pa·s and $a = 12$ cm. Hence, our rotation frequency yields stress levels that correspond those observed when considering physiological arterial pressure (6–40 dynes/cm²). HUVECs from the same passage, which were not subjected to shear stress, were kept in the same CO₂ incubator and were considered as static control.

2.5. Western blotting

After 72 h of subjecting to shear stress and responding to CoCr-

enriched medium, the challenged HUVECs were washed in ice-cold PBS and protein extracts were obtained using a RIPA lysis buffer (Sigma Aldrich, St. Louis, Missouri, USA), supplemented with a cocktail of anti-proteases and anti-phosphatases (Sigma Aldrich, St. Louis, Missouri, USA) up to 1 h on ice. Protein extracts were cleared by centrifugation 14,000 rpm for 15 min at 4 °C. The precipitate was then resuspended in 100 μ L of RIPA lysis buffer (Sigma Aldrich, St. Louis, Missouri, USA). The protein extracts were clarified and the protein concentration determined by the Lowry method [35]. Proteins extracts were resolved by SDS-PAGE and later transferred to PVDF membranes (Bio-Rad, Hercules, CA, USA). An equal volume of gel loading buffer [100 mmol L⁻¹ Tris-HCl (pH 6.8), 200 mmol L⁻¹ dithiothreitol (DTT), 4% SDS, 0.1% bromophenol blue, and 20% glycerol] was added to the samples and boiled for 5 min at 95 °C. Aliquots of the samples (75–100 μ g/lane) were resolved into SDS-PAGE (8, 10 or 12% gels) and later transferred to PVDF membranes (Millipore, USA), which were blocked with 5% nonfat dry milk dissolved in Tris-Buffered Saline (TBS)-Tween-20 (0.05%) and then incubated overnight with appropriate primary antibody (1:1,000) at 4 °C. After 1x-washing in TBS-Tween-20 (0.05%) and 2x-washing in TBS, the membranes were incubated with horseradish peroxidase-conjugated secondary anti-rabbit or anti-mouse IgGs antibodies (1:2,000), diluted in blocking buffer for 1 h. Immunoreactive bands were detected using Enhance Chemiluminescence (ECL, Pierce, USA).

2.6. mRNA isolation and RT-qPCR analysis

Challenged HUVECs were harvested properly and total mRNA isolated using Ambion TRIzol Reagent (Life Sciences-Fisher Scientific Inc., Waltham, MA, USA) and thereafter treated with DNase I (Invitrogen,

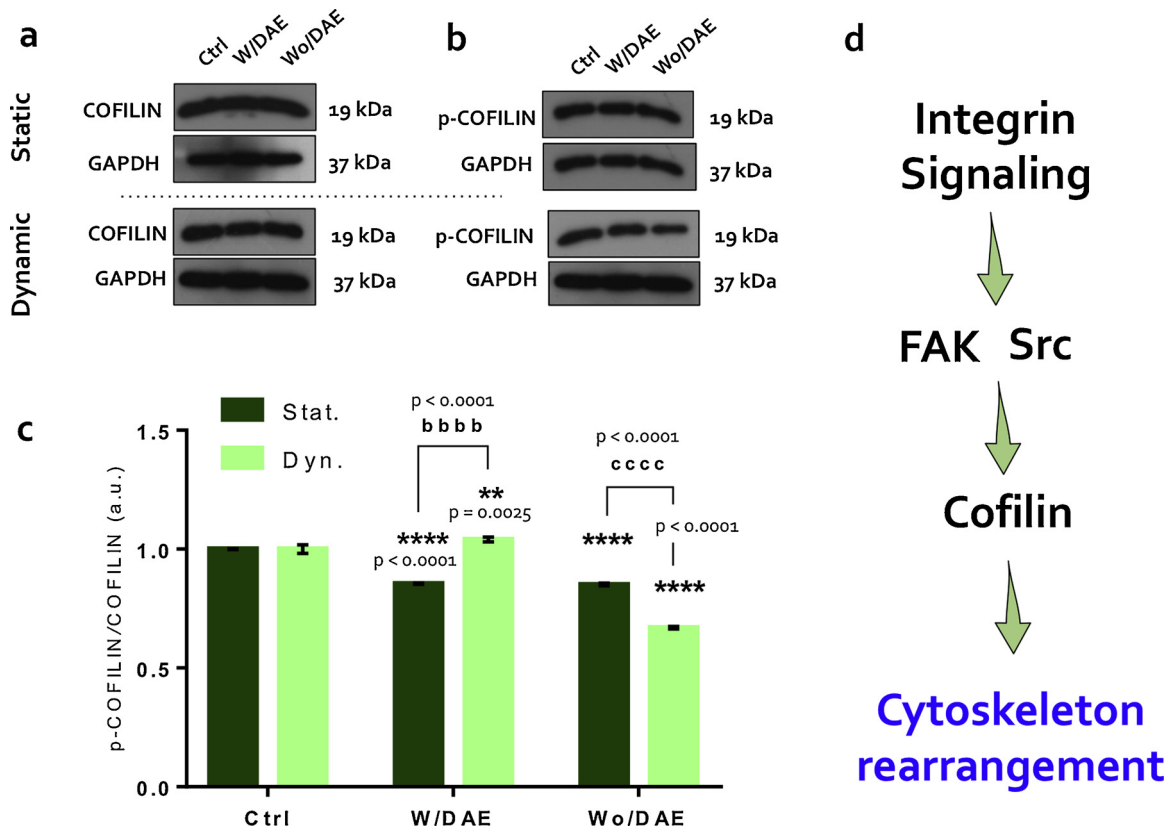


Fig. 2. Cytoskeleton dynamics. The phosphorylation of cofilin was evaluated in order to estimate cytoskeleton rearrangement dynamics: (a) cofilin, (b) p-cofilin and (c) representative blotting showing p-cofilin/cofilin ratio. Arbitrary values obtained by densitometry analyses of the bands are represented in the graphs. The letter “d” depicts on the signaling cascade required during cytoskeleton rearrangement. Significances were when: ***p* = 0.0025; ****p* < 0.0001. Results were represented as mean ± standard deviation of three independent experiments. The statistical analyses were performed by using two-way ANOVA, with further Sidak’s test for multiple comparisons (^{bbbb}*p* < 0.0001 and ^{cccc}*p* < 0.0001).

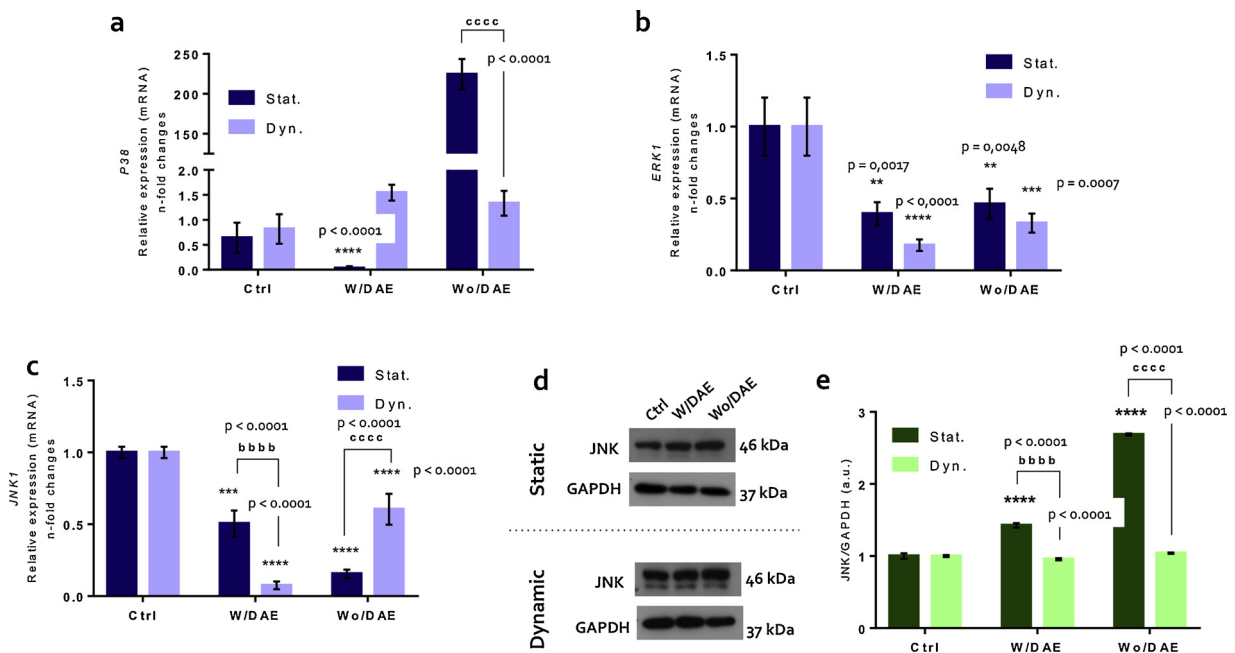


Fig. 3. MAPK member requirement in response to CoCr-enriched medium. Gene expression profile of MAPK signaling-related members [(a) P38, (b) ERK1 and (c) JNK1] was evaluated by RT-qPCR technology, and GAPDH, β-Actin and 18S were used as reference genes. Statistics were performed using two-way ANOVA, and Sidak’s test for comparison the effects of different surfaces (w/DAE and wo/DAE) with shear-stress (*p* values are displayed in the graphs).

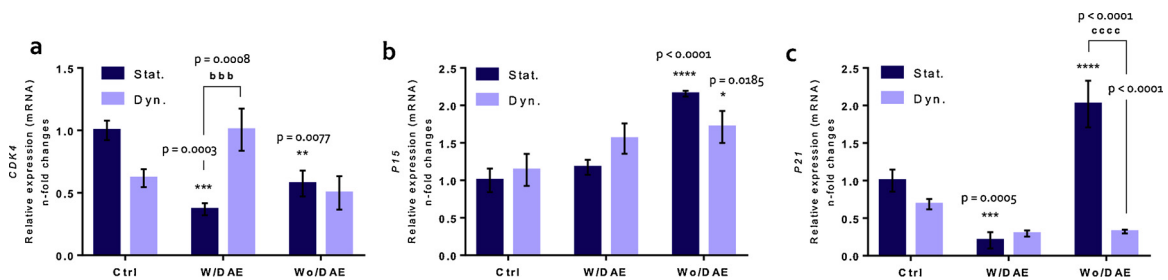


Fig. 4. Cell cycle members. RT-qPCR was performed to evaluate gene expression of cell cycle members: (a) CDK4, (b) P21 and (c) P15 genes were evaluated and the statistics performed by two-way ANOVA with Sidak's test as a multiple comparison of effects of different surfaces with shear-stress. Significances were when compared to control group: “*”, and when compared the effects of different surfaces (w/DAE and wo/DAE) with shear-stress (represented by the letters “b” or “c”). Technically, the data was normalized by 03 references genes: GAPDH, actin- β and 18S.

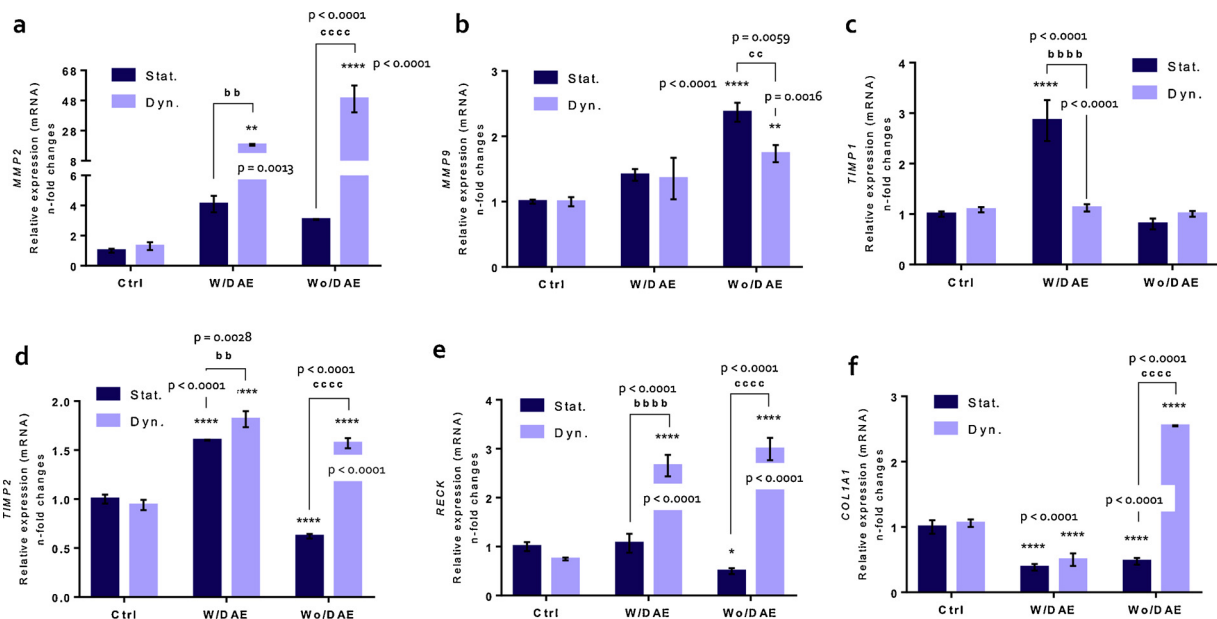


Fig. 5. Extracellular matrix remodeling. The extracellular remodeling was analyzed using RT-qPCR and zymography. (a) MMP2, (b) MMP9, (c) TIMP1, (d) TIMP2, (e) RECK and (f) COL1A1 mRNA profile expressions were evaluated and two-way ANOVA was performed to evaluate the significance of the data. Sidak's multiple comparison was also performed. Statistics: “*” shows the significances when the test groups were compared with the control, and letters “b” and “c” mean significances between different surfaces (w/DAE and wo/DAE) and shear-stress.

Carls-band, CA, USA). cDNA synthesis was performed with High Capacity cDNA Reverse Transcription Kit (Applied Biosystems, Foster City, CA, USA) according to the manufacturer's instructions. Real Time PCR was carried out in a total of 10 μ L, containing PowerUpTM SYBRTM Green Master Mix 2x (5 μ L) (Applied Biosystems, Foster City, CA, USA), 0.4 μ mol L⁻¹ of each primer, 50 ng of cDNA and nuclease free H₂O. Results were expressed as relative amounts of the transcripts using 3 internal reference genes (β -Actin, GAPDH and 18S genes) to better normalize the data obtained in the qPCR analysis (housekeeping gene), using the cycle threshold (ct) method. Primers and details are described in Table 1.

2.7. Zymography analyses

The proteolytic activities of both MMP-2 and MMP-9 presented in challenged HUVECs-conditioned medium were assayed by gelatin-based zymography, as described by Lefebvre [36]. Both static (control) and shear-stressed cultures were used to harvest those conditioned media, which they were after clarified by centrifugation 14,000 rpm for 15 min at 4 °C, and stored at -20 °C. In the moment of the analysis, the samples were quantified using the Lowry protein assay [35] and diluted in non-reducing buffer [0.1 mol L⁻¹ Tris-HCl, pH 6.8, 20% (v/v) glycerol, 1% (w/v) SDS and 0.001% (w/v) bromophenol blue]. Equal

amounts of protein (150 μ g) were loaded onto SDS-polyacrylamide gel [10% (w/v) and 4% (w/v) gelatin]. MMPs renaturation was performed in 2% (v/v) Triton X-100 overnight followed by the incubation in specific buffer [50 mmol L⁻¹ Tris-HCl and 10 mmol L⁻¹ CaCl₂ (pH 7.4)] at 37 °C overnight. Afterwards, gels were stained with 0.5% (w/v) Coomassie blue G 250 overnight, washed in a 30% (v/v) methanol and 10% (v/v) glacial acetic acid solution until the bands appear and then analyzed using software ImageJ.

2.8. Statistical analyses

Results were represented as mean \pm standard deviation (SD). The samples assumed a normal distribution with $p < 0.05$ considered statistically significant and $p < 0.001$ considered highly significant. In the experiment where there were > 2 groups, we used two-way ANOVA with multiple comparisons, in order to compare all pairs of groups. In this case, the significance level was considered when alpha = 0.05 (95% confidence interval). The software used was GraphPad Prism 7 (GraphPad Software, USA).

3. Results

In order to better analyze the effect of cobalt-chromium surfaces

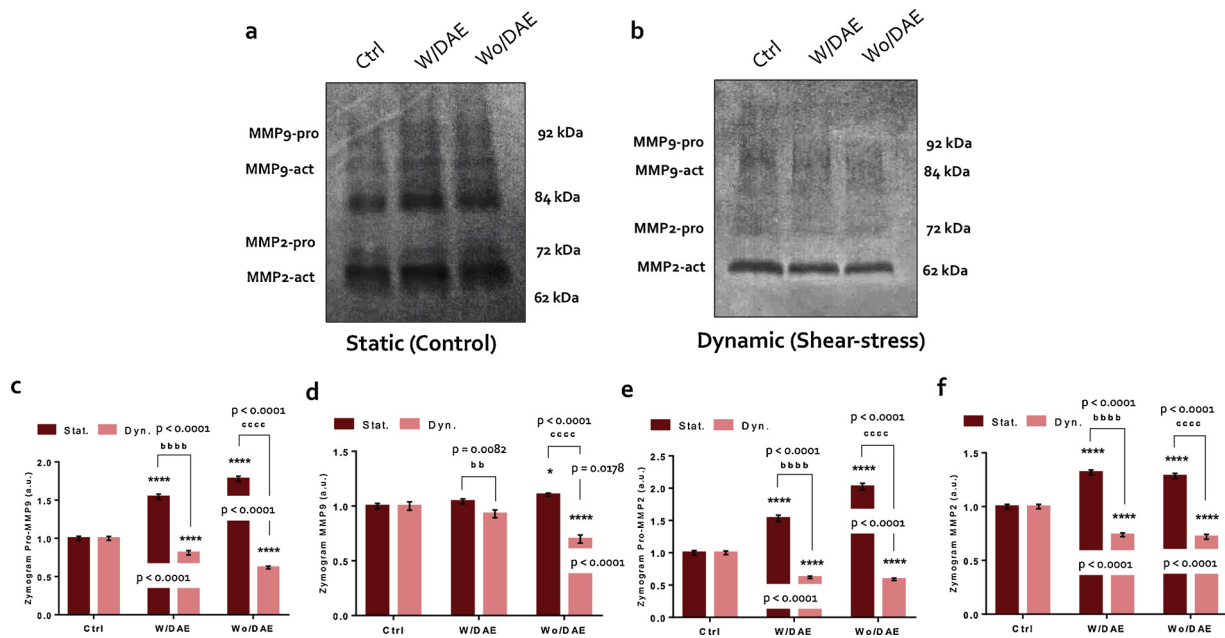


Fig. 6. Metalloproteinases activities were evaluated using Zymography. The activities of both MMP2 and MMP9 were analyzed using gelatin-containing gels. The zymogram depicting differences in (pro-)MMP-2 and (pro-)MMP-9 were shown (a, b; static and dynamic respectively). As detailed in material and methods, after activation step, the gel was stained with Coomassie blue by the methods outlined here. Two-way ANOVA with Sidak's multiple comparison test was used to compare the effects of different surfaces and shear-stress. The “*” shows the significance when compared to control group and the letters “b” and “c” show the statistical analyses when compared the effects of different surfaces (w/DAE and wo/DAE) with shear-stress.

(with or without DAE) on the shear-stressed endothelial cells, RT-qPCR and Western Blotting technologies were performed.

Firstly, intracellular pathways related with cell viability and survival was evaluated. The AKT (mRNA level) pattern was increased when endothelial cells were subjected to shear-stress (Fig. 1a). It seems shear-stress triggers survival signaling requiring the overexpression of AKT, when in response to CoCr, as well as FAK (mRNA level; Fig. 1b). Additionally, SRC mRNA profile was also responsive to CoCr, with positive interference of shear-stress condition, and presented a very similar pattern of expression to AKT (Fig. 1c). However, this immediate response to CoCr by reprogramming AKT and SRC genes did not reflect to the protein amount (Fig. 1d–g), suggesting any post-transcriptional mechanism to drive this response. Both of AKT and the Src proteins were higher in response to wo/DAE than others groups, but this profile was reduced considering shear stress.

As cytoskeleton rearrangement seems to be involved with cell viability in response to biomaterials, we decided to evaluate the profile of cofilin phosphorylation at Ser03, and the ratio of Cofilin phosphorylation was assessed in endothelial cells responding to the different groups using Western Blotting technology. The phosphorylation of cofilin was very dynamic considering both parameters: surface of materials and shear stress. Once again, shear-stress compromises the response to the CoCr (Fig. 2a–c). Mechanistically, the Fig. 2d depicts a probable intracellular pathway able to drive cofilin phosphorylation.

Thereafter, the MAPK reprogramming genes (P38, Erk1, JNK) were evaluated by RT-qPCR technology. Although our data shows significant changes on MAPK-P38 in response to the both w/DAE and wo/DAE (Fig. 3a), the presence of shear stress decreased this significance, suggesting an influence of autocrine mechanosignaling in response to the biomaterials. In addition, MAPK-ERK1 gene was significantly decreased in response to w/DAE and wo/DAE (Fig. 3b), here considering both static and dynamic conditions, and this pattern was also found for JNK (Fig. 3c). In relation to JNK, the amount of protein was also evaluated (Fig. 3d). Again, in both cases there are significances in the responses considering static and dynamic model, reinforcing the effect of shear-stress in this scenario. As it was evident the maintenance of survival signaling in response to the variations to present CoCr materials, we

decided to evaluate the reprogramming of genes related with cell cycle, looking for estimate mechanism involved with angiogenesis. Thus, the expressions of CDK4, P21 and P15 genes were also analyzed by RT-qPCR technology. CDK4 mRNA pattern was modulated by the presenting surface modifications (Fig. 4a), as well as to the shear-stress condition. Regarding both genes related with the arrest of cell cycle, both p15 and p21 genes were reprogrammed in response to the CoCr, with also interference of shear-stress in this response (Fig. 4b, c; respectively).

Considering the success of the endosseus implants ECM remodeling emerges as important pre-requisite to support bone *de novo* deposition and angiogenesis. In order to better address this issue, we evaluate the ECM remodeling in response to CoCr by investigating MMPs, at mRNA and activity levels, performing RT-qPCR and zymography respectively. Considering the transcriptional profile, MMP2 was significantly up-modulated in response to CoCr and sensible to the surfaces of the materials (Fig. 5a), as well as MMP9 (Fig. 5b). Complimentarily, we have also addressed the analysis of negative modulators of MMP's activity: TIMP1 (Fig. 5c), TIMP2 (Fig. 5d), and RECK (Fig. 5e). Important to report that all of them were differentially modulated respecting the surfaces of the materials, with a significant increase when they were compared with the control. Moreover, shear-stress exerts crucial relevance on the reprogramming of those genes activation (Fig. 5). Lastly, we have investigated whether collagen (col1A1) was modulated in response to CoCr and our qPCR data shows there is a significant up-expression of Col1A1 in response to wo/CoCr associated with shear-stress (Fig. 5f).

To better conclude on ECM remodeling in this context, we further analyzed the activity of MMP2 and MMP9 by performing gelatin-based zymography and the Fig. 6 brings an overall analysis, highlighting the activities of proMMPs and MMP at the active conformation (base on the molecular weight). Our data shows a differential activity of both MMPs2 (Fig. 6a, b, e, f) and 9 (Fig. 6a–d) comparing both surfaces investigated, it being increased on both cases when the static condition was considered; conversely, this activity was significantly down-modulated by shear-stressed endothelial cells. From our data it is clear that shear-stress signaling decrease the activities of MMPs in response

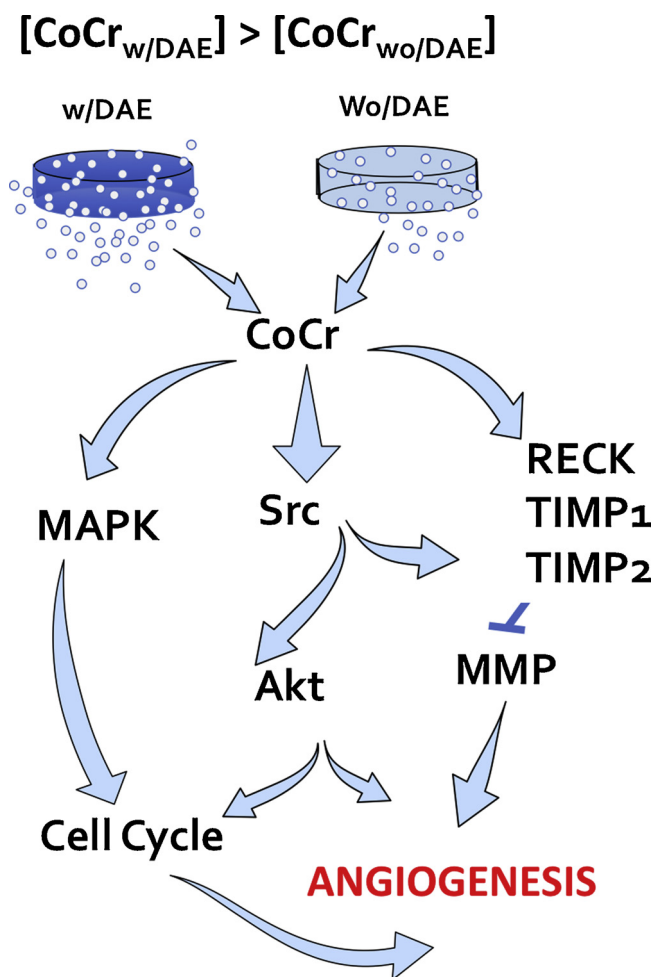


Fig. 7. Schematization of the main data obtained in this study. The trace of released CoCr triggers intracellular mechanism in endothelial cell requiring activation of MAPK pathway, Src, AKT, and these upstream members drive the signaling involved with cell cycle and ECM remodeling. Taken these data into account, it is possible to suggest an involvement of angiogenesis in response to CoCr.

to CoCr.

The Fig. 7 summarizes the mechanism suggested by the data obtained in this study. It is possible to suggest that survival signaling drives proliferative phenotype, as well as the ECM remodeling, in response to CoCr.

4. Discussion

Biomedical materials development is placed in an interdisciplinary field, which brings together engineering, physical-chemical and biological aspects, looking for accelerating the recovery of patient. Historically, titanium materials are considered the gold standard when looking for metal-based biomaterials focused on bone tissue repair in dentistry and medicine [3,15]. Despite the unquestionable biocompatibility of titanium, efforts have been worldwide focused on reducing the recovering time of the patients by enhancing the performance of biomaterial-related osseointegration [3]. In this sense, the proposal of novel biomaterials to be applied in biomedical field is very welcome, as well as modification of their surfaces are also relevant alternatives to enhance their performance when interacting with surrounding host tissue [3]. Based on this matter, other biomaterials than titanium have been proposed and CoCr and Zirconia have been emerged presenting important physicochemical and biological properties [16,37]. Although some progress is already reached in pre-clinical experimentation, there

is a lack on understanding their effects on endothelial cell performance. Recently, besides to the classical role of blood vessels in supporting cell metabolism away by supplying them with nutrients, there is now emerging evidences highlighting their cross-talk with bone cells [14]. Thus, considering the effect of biomaterials on endothelial cell metabolism and response seems being necessary, mainly when those biomaterials are proposed for bone injuries. In order to better address this issue, this study brings an experimental design considering the effect of CoCr-enriched medium on endothelial cell performance; these endothelial cells were also subjected to shear-stress to better mimic physiological condition of vascular biology.

Firstly, we have focused on evaluating the effect of CoCr on endothelial cell viability and survival pathway. Our data shows some effect on SRC and FAK, proteins involved in the integrin-based signaling pathway, which we have previously demonstrated being crucial to drive cell adhesion onto biomaterials surfaces [38]. Additionally, this involvement of Src seems to be important on participating with Akt pathway, a kinase responsible to the regulation of several central biological processes such as proliferation, survival, angiogenesis, among others [39]. Classically, changes in the levels of these proteins trigger signaling pathways related with cytoskeletal rearrangement, linking cytoskeleton proteins with cell survival processes [38,40,41]. Thus, to validate this hypothesis, we further evaluated the pattern of cofilin phosphorylation (at Serine 3). To date, cofilin is a cytoskeletal-related protein able to drive actin rearrangement by their capacity to interact with either actin monomers or F-actin according to the level of phosphorylation at the residue S3 [41,42]. Considering our experimental model, cofilin phosphorylation was sensible to the both surfaces evaluated here and this suggests an adaptation of the endothelial cytoskeleton when in response to those modifications of CoCr surfaces. Moreover, our data demonstrates that the interaction between surface modification and shear-stress are decisive external parameters to modulate gene expression and protein levels of Src, FAK and AKT, and of course driving endothelial cell viability. This mechanism also involves a dynamic participation of MAPKs in response to CoCr-enriched medium. To date, MAPK signaling is classically reported on driving intracellular signaling [43,44] and has been related with responses to different surfaces such as titanium, suggesting as a crucial step for cell survival and proliferation [45,46]. In conjunction, this set of results found corroborates with our previous published data, where we showed the effect of CoCr on osteoblasts and fibroblasts [16]. As experimental design, we have considered only an indirect effect of the surfaces on the cell metabolism, and the differential response of them to the variations on the surfaces of the materials (W/DAE and Wo/DAE) might be explained by the differential concentration of released elements to the extracellular compartment (here named CoCr-enriched medium); in fact, before treating the cells with, Fernandes et al (2018) measured the content of cobalt and chromium in the CoCr-enriched medium and the results surprisingly showed there is a significant increase on the amount of these released elements, quantified by graphite furnace technology [16].

Taken into account this panorama involving mechanism related with cell viability and survival, this prompted us to investigate the possibility of this CoCr-enriched medium in modulating endothelial cell growth. Considering the activation of CDK4 gene, our data shows that while CoCr-enriched medium seems decrease in a half the proliferative stimulus in the static condition, shear-stressed endothelial cells maintained it at a very similar profile of the control. In addition, this proliferating phenotype of endothelial cells in response to CoCr-enriched medium seems being modulated by p15 and p21 proteins [47,48], which they were found in this response. It is clear that our decision in considering shear-stressed cells was decisive to understand the real effect on endothelial performance, mainly because endothelial cells are considerate mechanosensitives and develop responses based on this phenotype. Importantly, the proliferating phenotype of endothelial cells is found in mechanism of angiogenesis and the modulation of this

process is expected for the success of osseointegration of implants within host tissue.

Finally, we analyzed the remodeling of the extracellular matrix by shear-stressed endothelial cell in response to CoCr-enriched medium, once ECM remodeling is reported as a crucial mechanism by favoring cell adhesion and viability during interaction with different biomaterials [19,37,49,50]. Importantly, our data report a significant and dynamic reprogramming of ECM remodeling-related gene and it seems there is an adequate balance of MMPs and their inhibitors genes. Again, the shear-stressed endothelial cells respond to the CoCr at differential manner. It is known that shear-stress is reported as a factor provoking ECM remodeling in endothelial cells [51]. Conversely, the CoCr promoted an increase on the MMP activity by static endothelial cells, while this pattern was significantly decreased in concomitant response to the shear-stress and this finding strongly suggest that CoCr does not exerts a direct effect on the MMP's activity. Overall in this case, it is expected that shear-stressed endothelial cells responding to CoCr present a reprogram of MMP's inhibitors responsible to this balance of their activities, as it can be observed in the gene expression of RECK, TIMP1, and TIMP2. Altogether, these results show that there is a fine control of ECM remodeling in response to CoCr, and the tensional forces of shear-stress drive this mechanism and this condition might reflect on angiogenesis. However, this mechanism requires novel strategies of analysis, maybe changing the intensity of these tensional forces, as it is found in the whole body.

Overall, our results demonstrate that CoCr-enriched medium affects shear-stressed endothelial cells favoring cellular mechanism required to angiogenesis and they bring the molecular basis to explain the biological relevance of CoCr as a promising biomedical device (Fig. 7). It is important to note that despite the wide knowledge about the influence of implants surface on bone cells, very little advance has been achieved on their effects considering endothelial cells. Additionally, the biological model used in this study is also something new in the field of biomaterials development and the consideration of shear-stressed cells guarantees a better mimicking of physiological responses and should be considered in further studies focusing on better understand the biological behavior in response to biomaterials.

Conflict of interest

None.

References

- N. An, A. Schedle, M. Wieland, O. Andrukhov, M. Matejka, X. Rausch-Fan, Proliferation, behavior, and cytokine gene expression of human umbilical vascular endothelial cells in response to different titanium surfaces, *J. Biomed. Mater. Res. – Part A* 93 (2010) 364–372, <https://doi.org/10.1002/jbm.a.32539>.
- C.J.C. Fernandes, F. Bezerra, M.R. Ferreira, A.F.C. Andrade, T.S. Pinto, W.F. Zambuzzi, Nano hydroxyapatite-blasted titanium surface creates a bionterface able to govern Src-dependent osteoblast metabolism as prerequisite to ECM remodeling, *Colloids Surf. B Biointerfaces* 163 (2018) 321–328, <https://doi.org/10.1016/j.colsurfb.2017.12.049>.
- P.G. Coelho, J.M. Granjeiro, G.E. Romanos, M. Suzuki, N.R.F. Silva, G. Cardaropoli, V.P. Thompson, J.E. Lemons, Basic research methods and current trends of dental implant surfaces, *J. Biomed. Mater. Res. B Appl. Biomater.* 88 (2009) 579–596, <https://doi.org/10.1002/jbm.b.31264>.
- V. Sabaliauskas, R. Juciute, V. Bukelskiene, V. Rutkunas, R. Trumpaite-Vanagiene, A. Puriene, In vitro evaluation of cytotoxicity of permanent prosthetic materials, *Stomatologija* 13 (2011) 75–80.
- B. Behl, I. Papageorgiou, C. Brown, R. Hall, J.L. Tipper, J. Fisher, E. Ingham, Biological effects of cobalt-chromium nanoparticles and ions on dural fibroblasts and dural epithelial cells, *Biomaterials* 34 (2013) 3547–3558, <https://doi.org/10.1016/j.biomaterials.2013.01.023>.
- A. Kanaji, V. Orhue, M.S. Caicedo, A.S. Virdi, D.R. Sumner, N.J. Hallab, T. Yoshiaki, K. Sena, Cytotoxic effects of cobalt and nickel ions on osteocytes in vitro, *J. Orthop. Surg. Res.* 9 (2014) 91, <https://doi.org/10.1186/s13018-014-0091-6>.
- D.L. Cochran, D. Buser, C.M. Ten Bruggenkate, D. Weingart, T.M. Taylor, J.P. Bernard, F. Peters, J.P. Simpson, The use of reduced healing times on ITI® implants with a sandblasted and acid-etched (SLA) surface: early results from clinical trials on ITI® SLA implants, *Clin. Oral Implants Res.* 13 (2002) 144–153, <https://doi.org/10.1034/j.1600-0501.2002.130204.x>.
- J.S. Suwandi, R.E.M. Toes, T. Nikolic, B.O. Roep, Biomechanical evaluation of the interfacial strength of a chemically modified sandblasted and acid-etched titanium surface, *Clin. Exp. Rheumatol.* 33 (2015) 97–103, <https://doi.org/10.1002/jbm.a>.
- C. Masaki, G.B. Schneider, R. Zaharias, D. Seabold, C. Stanford, Effects of implant surface microtopography on osteoblast gene expression, *Clin. Oral Implants Res.* 16 (2005) 650–656, <https://doi.org/10.1111/j.1600-0501.2005.01170.x>.
- B. Shi, O. Andrukhov, S. Berner, A. Schedle, X. Rausch-Fan, The angiogenic behaviors of human umbilical vein endothelial cells (HUVEC) in co-culture with osteoblast-like cells (MG-63) on different titanium surfaces, *Dent. Mater.* 30 (2014) 839–847, <https://doi.org/10.1016/j.dental.2014.05.005>.
- B. Of, W. Healing, *Inter-Leukin-1, Transforming Growth Factor*, (1999).
- M.A. Saghiri, A. Asatourian, F. Garcia-Godoy, N. Sheibani, The role of angiogenesis in implant dentistry part I: review of titanium alloys, surface characteristics and treatments, *Med. Oral Patol. Oral y Cir. Bucal.* 21 (2016) e514–e525, <https://doi.org/10.4317/medoral.21199>.
- J. Ando, K. Yamamoto, Effects of shear stress and stretch on endothelial function, *Antioxid. Redox Signal.* 15 (2011) 1389–1403, <https://doi.org/10.1089/ars.2010.3361>.
- S.K. Ramasamy, A.P. Kusumbe, M. Schiller, D. Zeuschner, M.G. Bixel, C. Milia, J. Gamrekelashvili, A. Limbourg, A. Medvinsky, M.M. Santoro, F.P. Limbourg, R.H. Adams, Blood flow controls bone vascular function and osteogenesis, *Nat. Commun.* 7 (2016) 1–13, <https://doi.org/10.1038/ncomms13601>.
- S. Gemini-Piperni, E.R. Takamori, S.C. Sartoretto, K.B.S. Paiva, J.M. Granjeiro, R.C. de Oliveira, W.F. Zambuzzi, Cellular behavior as a dynamic field for exploring bone bioengineering: a closer look at cell-biomaterial interface, *Arch. Biochem. Biophys.* 561 (2014) 88–98, <https://doi.org/10.1016/j.abb.2014.06.019>.
- C.J.C. Fernandes, F. Bezerra, M. das, D. do Carmo, G.S. Feltran, M.C. Rossi, R.A. da Silva, P. de, M. Padilha, W.F. Zambuzzi, CoCr-enriched medium modulates integrin-based downstream signaling and requires a set of inflammatory genes reprogramming in vitro, *J. Biomed. Mater. Res. A* 106 (2018) 839–849, <https://doi.org/10.1002/jbm.a.36244>.
- W.F. Zambuzzi, C.V. Ferreira, J.M. Granjeiro, H. Aoyama, Biological behavior of pre-osteoblasts on natural hydroxyapatite: a study of signaling molecules from attachment to differentiation, *J. Biomed. Mater. Res. A* 97 (2011) 193–200, <https://doi.org/10.1002/jbm.a.32933>.
- M.C. Rossi, F.J.B. Bezerra, R.A. Silva, B.P. Crulhas, C.J.C. Fernandes, A.S. Nascimento, V.A. Pedrosa, P. Padilha, W.F. Zambuzzi, Titanium-released from dental implant enhances pre-osteoblast adhesion by ROS modulating crucial intracellular pathways, *J. Biomed. Mater. Res. A* 105 (2017) 2968–2976, <https://doi.org/10.1002/jbm.a.36150>.
- F. Bezerra, M.R. Ferreira, G.N. Fontes, C.J. da Costa Fernandes, D.C. Andia, N.C. Cruz, R.A. da Silva, W.F. Zambuzzi, Nano hydroxyapatite-blasted titanium surface affects pre-osteoblast morphology by modulating critical intracellular pathways, *Biotechnol. Bioeng.* 114 (2017) 1888–1898, <https://doi.org/10.1002/bit.26310>.
- S. Chatterjee, A.B. Fisher, Mechanotransduction in the endothelium: role of membrane proteins and reactive oxygen species in sensing, transduction, and transmission of the signal with altered blood flow, *Antioxid. Redox Signal.* 20 (2014) 899–913, <https://doi.org/10.1089/ars.2013.5624>.
- R.A. da Silva, C.J. da, C. Fernandes, G. da, S. Feltran, A.M. Gomes, A.F. de Camargo Andrade, D.C. Andia, M.P. Peppelenbosch, W.F. Zambuzzi, Laminar shear stress-provoked cytoskeletal changes are mediated by epigenetic reprogramming of TIMP1 in human primary smooth muscle cells, *J. Cell. Physiol.* (2018), <https://doi.org/10.1002/jcp.27374>.
- K.D. Mahajan, G.M. Nabar, W. Xue, M. Anghelina, N.I. Moldovan, J.J. Chalmers, J.O. Winter, Mechanotransduction effects on endothelial cell proliferation via CD31 and VEGFR2: implications for immunomagnetic separation, *Biotechnol. J.* 12 (2017) 1600750, <https://doi.org/10.1002/biot.201600750>.
- B.D. Johnson, K.J. Mather, J.P. Wallace, Mechanotransduction of shear in the endothelium: basic studies and clinical implications, *Vasc. Med.* 16 (2011) 365–377, <https://doi.org/10.1177/1358863X11422109>.
- B.M. Mazzag, J.S. Tamaresis, A.I. Barakat, A model for shear stress sensing and transmission in vascular endothelial cells, *Biophys. J.* 84 (2003) 4087–4101.
- Y.-S.J. Li, J.H. Haga, S. Chien, Molecular basis of the effects of shear stress on vascular endothelial cells, *J. Biomech.* 38 (2005) 1949–1971, <https://doi.org/10.1016/j.jbiomech.2004.09.030>.
- C.G. Galbraith, R. Skalak, S. Chien, Shear Stress Induces Spatial Reorganization of the Endothelial Cell Cytoskeleton 330 (1998), pp. 317–330.
- X. Gong, X. Zhao, B. Li, Y. Sun, M. Liu, Y. Huang, X. Jia, J. Ji, Y. Fan, Quantitative studies of endothelial cell fibronectin and filamentous actin (F-Actin) coilignment in response to shear stress, *Microsc. Microanal.* 23 (2017) 1013–1023, <https://doi.org/10.1017/S1431927617012454>.
- S. Noria, D.B. Cowan, A.I. Gotlieb, B.L. Langille, Transient and Steady-State Effects of Shear Stress on Endothelial Cell Adherens Junctions, (1999), pp. 504–514.
- S. Li, M. Kim, Y. Hu, S. Jalali, D.D. Schlaepfer, T. Hunter, S. Chien, J.Y. Shyy, Fluid shear stress activation of focal adhesion kinase, *J. Biol. Chem.* 272 (1997) 30455–30462.
- E. Tzima, M.A. del Pozo, S.J. Shattil, S. Chien, M.A. Schwartz, Activation of integrins in endothelial cells by fluid shear stress mediates Rho-dependent cytoskeletal alignment, *EMBO J.* 20 (2001) 4639–4647, <https://doi.org/10.1093/emboj/20.17.4639>.
- D.T. Tambe, C.C. Hardin, T.E. Angelini, K. Rajendran, D.A. Weitz, J.J. Fredberg, X. Trepate, Collective cell guidance by cooperative intercellular forces, *Nat. Mater.* 10 (2011) 469–475, <https://doi.org/10.1038/nmat3025>.
- T.S. Pinto, C.J. da Silva, C. Fernandes, R.A. da Silva, A.M. Gomes, J.C.S. Vieira, P. de M. Padilha, W.F. Zambuzzi, c-Src kinase contributes on endothelial cells

- mechanotransduction in a heat shock protein 70-dependent turnover manner, *J. Cell. Physiol.* 234 (2019) 11287–11303, <https://doi.org/10.1002/jcp.27787>.
- [33] R.A. da Silva, A.F. de Camargo Andrade, G. da Silva Feltran, C.J. da, C. Fernandes, R.I.F. de Assis, M.R. Ferreira, D.C. Andia, W.F. Zambuzzi, The role of triiodothyronine hormone and mechanically-stressed endothelial cell paracrine signalling synergism in gene reprogramming during hBMSC-stimulated osteogenic phenotype in vitro, *Mol. Cell. Endocrinol.* 478 (2018) 151–167, <https://doi.org/10.1016/j.mce.2018.08.008>.
- [34] N.G. dela Paz, T.E. Walshe, L.L. Leach, M. Saint-Geniez, P.A. D'Amore, Role of shear-stress-induced VEGF expression in endothelial cell survival, *J. Cell Sci.* 125 (2012) 831–843, <https://doi.org/10.1242/jcs.084301>.
- [35] E.F. Hartree, Determination of protein: a modification of the Lowry method that gives a linear photometric response, *Anal. Biochem.* 48 (1972) 422–427.
- [36] V. Lefebvre, C. Peeters-Joris, G. Vaes, Production of gelatin-degrading matrix metalloproteinases ('type IV collagenases') and inhibitors by articular chondrocytes during their dedifferentiation by serial subcultures and under stimulation by interleukin-1 and tumor necrosis factor alpha, *Biochim. Biophys. Acta* 1094 (1991) 8–18.
- [37] C.J. da Costa Fernandes, M.R. Ferreira, F.J.B. Bezerra, W.F. Zambuzzi, Zirconia stimulates ECM-remodeling as a prerequisite to pre-osteoblast adhesion/proliferation by possible interference with cellular anchorage, *J. Mater. Sci. Mater. Med.* 29 (2018), <https://doi.org/10.1007/s10856-018-6041-9>.
- [38] W.F. Zambuzzi, R. Milani, A. Teti, Expanding the role of Src and protein-tyrosine phosphatases balance in modulating osteoblast metabolism: lessons from mice, *Biochimie* 92 (2010) 327–332, <https://doi.org/10.1016/j.biochi.2010.01.002>.
- [39] V. Betapudi, M. Shukla, R. Alluri, S. Merkulov, K.R. McCrae, Novel role for p56/Lck in regulation of endothelial cell survival and angiogenesis, *FASEB J.* 30 (2016) 3515–3526, <https://doi.org/10.1096/fj.201500040>.
- [40] G.V.O. Fernandes, A.D.M. Cavagis, C.V. Ferreira, B. Olej, M. de S. Leao, C.L. Yano, M. Peppelenbosch, J.M. Granjeiro, W.F. Zambuzzi, Osteoblast adhesion dynamics: a possible role for ROS and LMW-PTP, *J. Cell. Biochem.* 115 (2014) 1063–1069, <https://doi.org/10.1002/jcb.24691>.
- [41] W.F. Zambuzzi, A. Bruni-Cardoso, J.M. Granjeiro, M.P. Peppelenbosch, H.F. de Carvalho, H. Aoyama, C.V. Ferreira, On the road to understanding of the osteoblast adhesion: cytoskeleton organization is rearranged by distinct signaling pathways, *J. Cell. Biochem.* 108 (2009) 134–144, <https://doi.org/10.1002/jcb.22236>.
- [42] Z. Ostrowska, J. Moraczewska, Cofilin - a protein controlling dynamics of actin filaments, *Postepy Hig. Med. Dosw.* 71 (2017) 339–351 (Online).
- [43] B.E. Slack, M.S. Siniaia, Adhesion-dependent redistribution of MAP kinase and MEK promotes muscarinic receptor-mediated signaling to the nucleus, *J. Cell. Biochem.* 95 (2005) 366–378, <https://doi.org/10.1002/jcb.20431>.
- [44] T. Gantke, S. Sriskantharajah, M. Sadowski, S.C. Ley, IkappaB kinase regulation of the TPL-2/ERK MAPK pathway, *Immunol. Rev.* 246 (2012) 168–182, <https://doi.org/10.1111/j.1600-065X.2012.01104.x>.
- [45] M. Cargnello, P.P. Roux, Activation and function of the MAPKs and their substrates, the MAPK-activated protein kinases, *Microbiol. Mol. Biol. Rev.* 75 (2011) 50–83, <https://doi.org/10.1128/MMBR.00031-10>.
- [46] E.K. Kim, E.-J. Choi, Pathological roles of MAPK signaling pathways in human diseases, *Biochim. Biophys. Acta* 1802 (2010) 396–405, <https://doi.org/10.1016/j.bbdis.2009.12.009>.
- [47] C.R. Geyer, Strategies to re-express epigenetically silenced p15(INK4b) and p21(WAF1) genes in acute myeloid leukemia, *Epigenetics* 5 (2010) 696–703, <https://doi.org/10.4161/epi.5.8.13276>.
- [48] A.L. Gartel, K. Shchors, Mechanisms of c-myc-mediated transcriptional repression of growth arrest genes, *Exp. Cell Res.* 283 (2003) 17–21.
- [49] C.J. da Costa Fernandes, F.J.B. Bezerra, B. de Campos Souza, M.A. Campos, W.F. Zambuzzi, Titanium-enriched medium drives low profile of ECM remodeling as a pre-requisite to pre-osteoblast viability and proliferative phenotype, *J. Trace Elem. Med. Biol.* 50 (2018) 339–346, <https://doi.org/10.1016/j.jtemb.2018.07.015>.
- [50] A. Marumoto, R. Milani, R.A. da Silva, C.J. da Costa Fernandes, J.M. Granjeiro, C.V. Ferreira, M.P. Peppelenbosch, W.F. Zambuzzi, Phosphoproteome analysis reveals a critical role for hedgehog signalling in osteoblast morphological transitions, *Bone* 103 (2017) 55–63, <https://doi.org/10.1016/j.bone.2017.06.012>.
- [51] R.E. Mott, B.P. Helmke, Mapping the dynamics of shear stress-induced structural changes in endothelial cells, *Am. J. Physiol. Cell Physiol.* 293 (2007) C1616–26, <https://doi.org/10.1152/ajpcell.00457.2006>.